

Effect of Thermal Diffusivity on the Detectability of TNDE

Junduo Zhao and Tsuchin Chu
Department of Mechanical Engineering and Energy Processes
Southern Illinois University at Carbondale
Carbondale, IL 62901-6603

Samuel S. Russell
Material Processes and Manufacturing Department
NASA/MSFC
Marshall Space Flight Center, AL 35812

ABSTRACT

The effect of thermal diffusivity on the defect detectability in Carbon/Epoxy composite panels by transient thermography is presented in this paper. A series of Finite Element Models were constructed and analyzed to simulate the transient heat transfer phenomenon during Thermographic Non-destructive Evaluation (TNDE) of composite panels with square defects. Six common carbon fibers were considered. The models were built for composites with various combinations of fibers and volumetric ratios. Finite Element Analysis of these models showed the trends of the detectable range and the maximum thermal contrast versus the thermal diffusivity of various composites. Additionally, the trends of defect size to depth ratio and the thermal contrast has been investigated.

Keywords: NDE, thermography, thermal diffusivity, thermal contrast, composite materials, FEA modeling.

1 INTRODUCTION

The area of non-destructive evaluation, or NDE, is one of the fastest growing areas in thermal wave research [1-7]. Non-destructive evaluation can be defined as the measurement, inspection, or analysis of materials and processes as part of a manufacturing or fabrication cycle. Modern manufacturing processes rely heavily on many measurements, inspections, and analyses. There is considerable interest in off-line process monitoring, in-line monitoring after a critical process step, and even *in-situ* monitoring during the actual process.

The method of FEA modeling and analysis has been used at NASA/MSFC since 1996 to help optimize the operation procedure of the TNDE testing system [8,9]. Methods of thermographic inspection could be modeled and compared based upon the FEM analysis thus reducing the number of physical tests required. Design good numerical models to represent defects and using FEA analysis help to reduce the production of real test parts which can be very time consuming and laborious.

There are many factors that have effects on the test capability of TNDE system. The most important one is the thermal diffusivity of the material. It has determining effect on the thermal contrast between the sound and defect material as well as the rising time to the maximum thermal contrast. In this paper, we pursue the goal of studying the effect of thermal diffusivity on the detection capability of TNDE system. Numerical finite element models of composite panels with simulated defect are generated and FEA software is employed to analyze these models. By this analysis the

effect of thermal diffusivity on the detection capability of the TNDE infrared thermography inspection systems is determined. To help fully understand the capability and range of the inspection system, a series of numerical finite element models of carbon/epoxy composite panels with different volume percentage of different fibers have been constructed and analyzed. The results are tabulated and the correlation between the thermal contrast, rising time and the thermal diffusivity of material is established. The results and the trends developed by this project will help understand the effect of thermal diffusivity and enhance the ability of determining the inspection parameters and capabilities for thermographic nondestructive evaluation (TNDE) of composite structures. Some laminated carbon/epoxy composite test panels with defects at various depth were built. Thermographic evaluation were performed on these panels and the temperature-time (T-t) curves were generated for comparison with the results obtained from the current finite element analysis. The problem of defect size/depth ratio was also studied. Different numerical FEA models of different defect size and depth but with same defect size/depth ratio were built. Results were analyzed and conclusion is drawn. The final goal is to establish proper procedures to provide the optimal thermal inspection protocol through analysis of the FEA results.

2 FINITE ELEMENT MODELING OF COMPOSITE PANELS WITH DEFECTS

Before any analysis could be performed, properties had to be found for several different materials. The main material property we concern about is thermal diffusivity, $\alpha = k / (\rho c)$, where k is the thermal conductivity, ρ is the density, and c is the specific heat. In this paper, the thermal conductivity, density and specific heat of the composite material are calculated by the rule of mixture.

Thermal properties and density of six different carbon fibers manufactured by Amoco were found. The thermal conductivity k for these fibers ranges from 22 to 640 W/m-K, giving us a diverse sample.

Thermal diffusivity α is defined by $k / \rho c$. Rules of mixture are used and results are obtained. α_x is the thermal diffusivity along the fiber and α_y is thermal diffusivity perpendicular to the fiber. Only 30%, 50% and 70% fiber volume percent are used. Epoxy resin (matrix) is the same for all models.

Quarter symmetry is used in the study to represent the panel with the defect. A typical finite element model of a composite panel with a square defect (quarter symmetry) is shown in Figure 1.

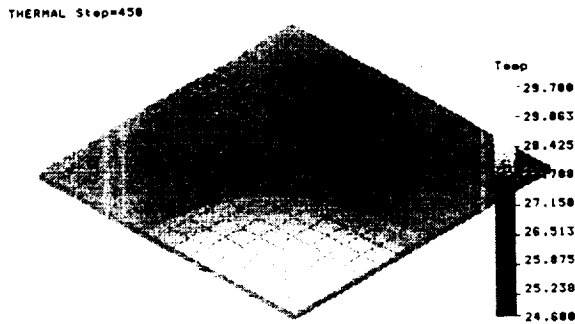


Figure 1. Finite element model of a square defect (defect size is 5 by 5 elements)

Next is to generate thermal contrast contour maps for various materials and create database for thermal contrast vs. material properties. The thermal contrast (C) on the surface of the panel is the temperature difference taken between two points on the surface of the model at any time step. The center of the defect (T_{def}) has the highest temperature and the outer sound region of the model (T_{sound}) has the lowest temperature. The computation of the thermal contrast is given by

$$C(t) = T_{\text{def}}(t) - T_{\text{sound}}(t) \quad (1)$$

The variable t is introduced because thermal contrast is a function of time. Figure 2 shows the T - t curves of the defect and sound areas. The difference in temperature is the thermal contrast.

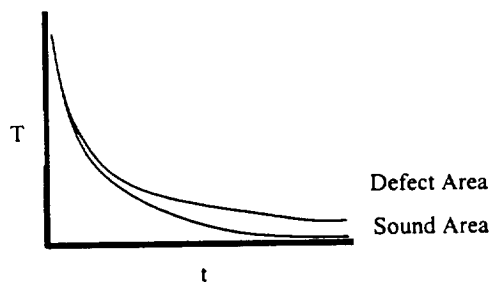


Figure 2. Temperature-time plot of defect and sound areas

The FEA software generates the Temperature vs. time (T - t) relation in a tabulated format. This tabulated information is exported manually to notepad as a text file and then imported to Microsoft Excel in a workbook. Next step is to calculate maximum temperature difference (thermal contrast) on the top surface and generate thermal contrast contour maps. After collecting enough data, a relation between the temperature difference and thermal diffusivity is established.

3 RESULTS AND DISCUSSION

The effect of thermal diffusivity on the heat transfer of the model gives extremely useful information about the behavior of the heat transport in the composite material. This provides a very helpful guide to the operator of the TNDE system to help predict the right time to catch the maximum thermal contrast and save time and effort. In the following, 6 series of models made from same matrix but different fibers are built and analyzed.

3.1 Finite Element Models and Boundary Conditions

The effect of thermal diffusivity is studied by varying the fiber contents and subsequently varying the material properties. The value of heat flux used for all sets of models is 1400 kW/m^2 . For each of the sets, 3 different volume percent (30, 50 and 70) are modeled. They have the same defect locations between 3rd and 4th ply, and they all are generated with a [0/90/0]_s laminate geometry. The size of the models is $38 \times 38 \text{ mm}$. The thickness of each ply is 0.15 mm for the models. The element used is an 8-node isoparametric solid element (brick element). Each element is one ply thick and there are 5 elements for every quarter-inch of length in most models. The time duration under investigation is 5 seconds and the time between each step is 0.002 seconds. The coefficient of natural convection applied to the top surface is $58.9 \text{ W/m}^2 \cdot ^\circ\text{C}$. The initial and ambient temperature of the composite is 24°C . The density, specific heat and thermal conductivity (in the direction perpendicular to the fiber and through the thickness) used for the finite element models of composite panels are calculated using rules of mixture.

3.2 Analysis of 3-ply Models

The relation between thermal diffusivity versus rising time and peak thermal contrast is obtained. All the data from the 3-ply models are collected and analyzed (Table 1).

Fiber %	α_x ($10^{-6} \text{ m}^2/\text{s}$)	Rising Time (sec)	Max. Thermal Contrast ($^\circ\text{C}$)
P120-30%	97.5	0.84	1.83
50%	176.6	0.54	1.88
70%	271.0	0.3	2.28
P100-30%	79.3	0.9	2.00
50%	144.0	0.6	2.08
70%	221.6	0.36	2.52
P75-30%	28.5	1.2	2.63
50%	52.1	0.78	2.90
70%	80.6	0.48	3.42
P55-30%	18.9	1.32	2.77
50%	34.6	0.9	3.13
70%	54.0	0.54	3.70
P25-30%	3.6	1.62	2.87
50%	6.5	1.2	3.31
70%	10.1	0.78	3.89
T50-30%	11.0	1.44	2.90
50%	20.5	0.96	3.38
70%	32.6	0.54	4.05

Table 1. Rising time and maximum thermal contrast (all 3-ply models)

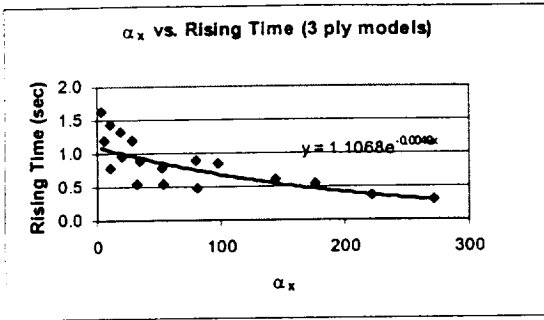


Figure 3. Thermal diffusivity α_x versus rising time (all 3-ply models)

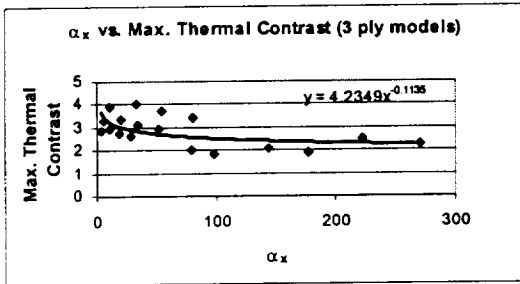


Figure 4. Thermal diffusivity α_x versus maximum thermal contrast (all 3-ply models)

From the data we find that the rising time is overall shorter when α_x is higher. The relation between α_x and the rising time follows a power function as shown in Figure 3. On the other hand, different from the relation found with each set of models, the maximum thermal contrast is smaller when α_x is higher. The relation between α_x and the maximum thermal contrast follows an exponential function as the trend line shows (Figure 4). To further investigate this conclusion, the other 6 series of models in which defect is located at the 4th ply are built and analyzed. The results show that the trend is very similar and the constants for the power and exponential functions are very close.

3.3 Comparing Data with Previous Experimental and Numerical Results

From previous experimental results (3-ply deep defect, IM6/3501-6 Graphite/Epoxy panel, 70% fiber contents) for a panel that has a thermal diffusivity of $5.28 \times 10^{-6} \text{ m}^2/\text{s}$ and uses a heat flux of 1400 kW, the rising time is 0.8 seconds and the maximum thermal contrast is 3.0°C [8]. The experimental results are compared to the data calculated from the 3-ply models trend line equation. The comparison of data is tabulated in Table 2. As can be seen in this table, the trend line can be used to predict very closely the rising time and the thermal contrast for a giving sets of conditions including the material properties and the defect characteristics.

$\alpha = 5.28 \times 10^{-6} \text{ m}^2/\text{s}$	Rising Time (sec)	Thermal Contrast ($^\circ\text{C}$)
Experimental Results	0.8	3
Calculated Results	0.97	3.5

Table 2. Comparison with experimental results

From previous numerical FEA results for a panel having very high thermal diffusivity, $\alpha_x = 1203.8 \times 10^{-6} \text{ m}^2/\text{s}$, that is subjected to a heat flux of 1400 kW, the rising time is 0.006 seconds and the maximum thermal contrast is 2.4°C . The data is compared to the results from the 3-ply model trend line equation (Table 3).

$\alpha = 1203.8 \times 10^{-6} \text{ m}^2/\text{s}$	Rising Time (sec)	Thermal Contrast ($^\circ\text{C}$)
Previous FEA Results	0.006	2.4
Calculated Results	0.003	1.9

Table 3 Comparison of data with previous FEA results

Notice that the experimental panel and numerical FEA model used in comparison have very low and high thermal diffusivity values respectively. The fact that the trend line can predict both the rising time and the thermal contrast to the same order of magnitude for panels with extreme thermal properties has proved that the FEA models and database generated is very useful in determining the detectability of TNDE.

From the results of analyzing a set of finite element models with various defect depths, we obtain a relation between thermal contrast and depth of the defect (Figure 5):

$$T = 1.1047 d^{-1.9112} \quad (2)$$

where T is the maximum thermal contrast in $^\circ\text{C}$ and d is the defect depth in mm.

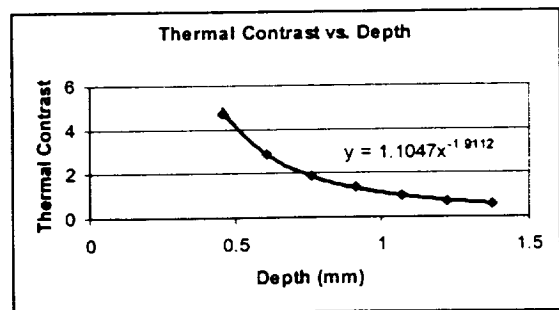


Figure 5. Thermal Contrast vs. Depth

Recall the trend line equation from 3-ply models (Figure 4):

$$T = 4.2349 \alpha^{-0.1135} \quad (3)$$

The effect of both thermal diffusivity and the defect depth on thermal contrast for a panel with the same defect size can be obtained by using equations 2 and 3:

$$T = 0.69 \alpha^{-0.1135} d^{-1.9112} \quad (4)$$

The above equation can be used as a tool for predicting thermal contrast in a panel.

3.4 Study of Defect Size/Depth Ratio Problem

Industry has an impression that defects with different size and different depth but same size/depth ratio might have same thermal characteristics. In this part, 3 FEA models are made and results are analyzed to demonstrate the possible relation.

All 3 models have the same defect size/depth ratio. Defects are located at 3rd, 4th and 5th ply.

The results show that although the temperature development is very close, the rising time and thermal contrast are quite different. The rising time and thermal contrast for different models are tabulated below:

	Side Length of Defect (mm)	Depth of Defect (mm)	Size/Depth Ratio	Rising Time (sec)	Thermal Contrast (°C)
Model 1	7.62	0.4572	16.67	0.66	1.8
Model 2	10.16	0.6096	16.67	0.96	1.11
Model 3	12.7	0.762	16.67	1.26	0.49

Table 4. Rising Time and Thermal Contrast for Different Models

From the data we can tell that when the defect is deeper, the rising time is longer and thermal contrast is lower. The trend is almost linear and it appears that the depth of the defect is the main factor that determines the rising time and the thermal contrast.

4 CONCLUSIONS

The effect of thermal diffusivity on the detectability range of TNDE as an FEA modeling problem has been presented. The problem of size/depth ratio was also discussed. Various models (defect at 3ply and 4 ply deep) have been built and results have been analyzed. The models were built with different material properties. They were also built with different defect size and depth but with the same size/depth ratio.

The study of the effect of thermal diffusivity (defect at 3-ply deep) indicates that there is an overall trend that the rising time becomes shorter when thermal diffusivity along fiber direction, α , becomes higher. The trend follows an exponential function, $y=1.1068e^{-0.049x}$, which means that the rising time will continuously become shorter if the thermal diffusivity keeps rising. The study of 3-ply models also indicates that there is an overall trend that the thermal contrast

becomes lower when thermal diffusivity along fiber direction becomes higher. The trend follows a power function (Equation 3), which means that when the thermal diffusivity is high enough, the thermal contrast will stop dropping. The results are verified by another set of 4-ply models.

The results were also verified by comparing the results with previous experimental and numerical FEA analysis results. Combining the results from present research and previous models, we get a trend line equation combine thermal diffusivity and defect depth (Equation 4). We can use this approach as a tool in the future to compare the experimental or FEA results as well as obtaining more generalized equations to include other possible parameters.

The problem of size/depth ratio was also studied. The analysis indicates that when depth of defect becomes deeper, the rising time becomes longer although they have same size/depth ratio. Thermal contrast also drops when the defect becomes deeper. The conclusion appears to be that the depth of defect is the main factor of determining the rising time and thermal contrast.

REFERENCES

1. Winfree, W., and Heath, D.M., "Thermal Diffusivity Imaging of Aerospace Materials and Structures," Thermosense XX, Proceedings of SPIE, Vol. 3361, 1998, pp. 282-290.
2. Sun, J.G., and Ellingson, W.A., "Thermal Characterization - An NDE Method for CFCCs," CFCC News, DOE Office of Industrial Technologies, May 1998, No. 10, pp.3-5.
3. Green, D.R., "Thermal and Infrared Nondestructive Testing of Composites and Ceramics," Materials Evaluation, Nov. 1971, pp. 241-248.
4. Vavilov, V., et. al., "Thermal Nondestructive Testing of Carbon Epoxy Composites: Detail Analysis and Data Processing," NDT & E International, Vol. 26, No. 2, 1993, pp. 85-95.
5. Connolly, M., and Copley, D., "Thermographic Inspection of Composite Materials," Materials Evaluation, Vol. 48, No. 12, Dec. 1990, pp 1461-1463.
6. Cramer, K. E., Syed, H. I. and Winfree, W. P., "Thermographic detection of cracks in thin sheets," Review of Progress in Quantitative Nondestructive Evaluation, edited by Thompson, D. O. and Chimenti, D. E., Vol. 10A, pp. 1087-1094, 1991.
7. Cramer, K. E., Winfree, W. P., "The application of Thermal Diffusivity Imaging to SIC Fiber Reinforced Silicon Nitride," Review of Progress in Quantitative Nondestructive Evaluation, edited by Thompson D. O. and Chimenti D. E., Vol. 12B, pp. 1305-1311, 1993.
8. Chu, T.C., DiGregorio, A.M., and Russel, S.S., "Determination of Experimental Parameters for Transient Thermography," Proceedings of the SEM Annual Conference on Theoretical, Experimental, and Computational Mechanics, June 7-9, 1999, pp. 318-321.
9. Brady, R.P., Kulkarni, M.R., Chu, T.C., and Russell, S.S., "Thermal Image Analysis for the on-line NDE of Composites," Proceedings of the Second Conference on NDE Applied to Process Control of Composite Fabrication, St. Louis, NTIAC-PR-97-01, pp. 123-136, 1996.